Controllable Coefficient Integrator Using Switching Operation

Controllable Coefficient Integrator Using Switching Operation

Isao MIZOSHIRI*, Suemitsu MINAMOTO** and Kazuo MIYAKOSHI**

(Received November 15, 1971)

This paper deals with principles and applications of a controllable coefficient integrator using switching operation. Filters of controllable parameters can be obtained by well using the controllable coefficient integrator. The filter is constructed with the integrator and switch connected in series to its input terminal. The coefficient of integration is controlled with the external control signal which controls on-off of switch.

Principles of the controllable coefficient integrator are mentioned and errors of the circuit are discussed in detail. The construction of controllable parameter filter is one of the most useful applications of the controllable coefficient integrator. The experimental results of the low pass filter of controllable cut-off frequency, the band pass filter of controllable center frequency and the auto frequency analyser are discussed.

1. Introduction

The controllable coefficient integrator has been built by using an integrator and a multiplier. The Miller integrator with a series switch in its input terminal shows the characteristics of the controllable coefficient integrator.

The switch repeats on-off in higher frequency compared with the frequency of the input signal of the integrator, and the ratio of on-time to repetition period is contolled by the external control signal. The relation between the integration coefficient and the external signal is kept in the same relation between the conducting interval (on-time) and the external signal. This relation may be chosen voluntarily not to mention linear relation.

This controllable coefficient integrator can be recognized as the combination circuit of Miller integrator and the time-sharing type multiplier. By combining with Miller integrator, the smoothing low pass filter can be eliminated from the time-sharing type multiplier.

Principles of operation, error discussion and applications of this controllable coefficient integrator is described.

2. Principles and circuit analysis

Fig. 1 shows the fundamental circuit of the controllable coefficient integrator. As the relation between the external control signal voltage $e_c(t)$ and the coefficient of integration is kept linear, on-off repetition of the switch S_w is controlled by the rectangular pulse $\kappa_s(t)$ whose width is modulated by the external control signal voltage $e_c(t)$. The average value of the input current to the operational amplifier is in proportion to both the input signal voltage $e_{in}(t)$ and the external control signal voltage $e_c(t)$. The output signal voltage $e_{out}(t)$

* Graduate Student, Department of Electronics, College of Engineering.
** Department of Electronics, College of Engineering.

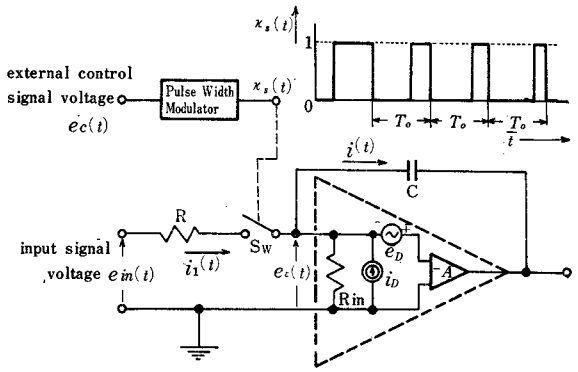

Fig. 1 Fundamental construction of controllable coefficient integrator

is obtained as the integrated value of $e_c(t)\cdot e_{in}(t)$. When the frequency range of external control signal voltage $e_c(t)$ is limited in much lower frequency range compared with that of $e_{in}(t)$, the coefficient of integration can be controlled by external control signal voltage $e_c(t)$. Using notations of Fig. 1 and applying Kirchhoff's laws, next four equations are derived.

$$e_\epsilon(t)=\{i_1(t)-i(t)+i_D(t)\}R_{in} \tag{1}$$

$$e_{out}(t)=-A\{e_\epsilon(t)+e_D(t)\} \tag{2}$$

$$e_\epsilon(t)-e_{out}(t)=\frac{1}{C}\int_{-\infty}^{t}i(t)dt \tag{3}$$

$$i_1(t)=\frac{1}{R}\{e_{in}(t)-e_\epsilon(t)\}\kappa_s(t) \tag{4}$$

From Eqs. (1)$\sim$(4), the output signal voltage $e_{out}(t)$ is obtained as follows;

$$e_{out}(t)=\frac{-1}{CRA(1+1/A)}\int_{-\infty}^{t}\Phi(t')\cdot e_{out}(t')dt'+u_1(t)+u_2(t)+u_3(t) \tag{5}$$

where

$$\Phi(t')=\kappa_s(t')+R/R_{in} \tag{6}$$

$$u_1(t)=\int_{-\infty}^{t}\frac{1}{CR(1+1/A)}e_{in}(t')\kappa_s(t')dt' \tag{7}$$

$$u_2(t)=\int_{-\infty}^{t}\frac{1}{CR(1+1/A)}\{\Phi(t')e_D(t)+Ri_D(t)\}dt \tag{8}$$

$$u_3(t)=\frac{-1}{(1+1/A)}e_D(t) \tag{9}$$

Eq. (5) is Volterra type integral equation of the second kind[1] and its solution is given as next Eq. (10).

$$e_{out}(t)=u_1(t)+u_2(t)+u_3(t)$$
$$+\sum_{n=1}^{\infty}\left\{\frac{-1}{CRA(1+1/A)}\right\}^n\int_{-\infty}^{t}\Phi_n(t,t')\{u_1(t')+u_2(t')+u_3(t')\}dt' \tag{10}$$

where

$$\left.\begin{aligned}\Phi_1(t,t') &= \Phi(t') \\ \Phi_n(t,t') &= \int_{t'}^{t} \Phi(t'')\cdot\Phi_{n-1}(t'',t)dt'', \qquad (n=2,3,\cdots)\end{aligned}\right\} \tag{11}$$

From Eqs. (8), (9), it is clear that $u_2(t)$, $u_3(t)$ are composed of drift and off-set components and they can be reduced to zero by means of proper compensations and adjustments. In general, the operational amplifier, for the integrator, is used under the condition of $ACR \gg 1$, and infinitive series of Eq. (10) is approximated to the first term.

$$\begin{aligned}e_{out}(t) &= \int_{-\infty}^{t} \frac{-1}{CR} e_{in}(t)\kappa_s(t)dt \\ &+ \frac{1}{(CR)^2 A}\int_{-\infty}^{t}\int_{-\infty}^{t'} \{\kappa_s(t') + R/R_{in}\} e_{in}(t'')\kappa_s(t'')dt''dt'\end{aligned} \tag{12}$$

Where $\kappa_s(t)$ is the switching function and its value takes unit while the switch S_w is conducting and zero while it is cutting off. $\kappa_s(t)$ may be recognized as the unit-amplitude rectangular pulse width modulated wave whose leading edge is modulated by the external control signal voltage $e_c(t)(\geqq 0)$ and it is represented by next Eq. (13).

$$\begin{aligned}\kappa_s(t) &= \frac{M}{T_0} e_c(t) + \sum_{\substack{m=-\infty \\ m\neq 0}}^{\infty} j\frac{1}{2m}\{1 - e^{j(2\pi/T_0)mMe_c(t)}\} e^{j(2\pi/T_0)mt} \\ &= \frac{M}{T_0} e_c(t) + \sum_{m=1}^{\infty}\frac{1}{m}\left[-\sin\frac{2\pi}{T_0}mt + \sin\frac{2\pi}{T_0}m\{Me_c(t)+t\}\right]\end{aligned} \tag{13}$$

Where $1/T_0$ is the repetition frequency of the switch and M is the arbitrary constant which represents modulation degree and satisfies

$$Me_c(t) \leqq T_0 \tag{14}$$

Using Eq. (13), Eq. (12) is rewritten as follows;

$$e_{out}(t) = -\frac{1}{CR}\cdot\frac{M}{T_0}\int_{-\infty}^{t} e_c(t)e_{in}(t)dt - \frac{1}{CR}\Delta_1(t) + \frac{1}{(CR)^2 A}\Delta_2(t) \tag{15}$$

The first term of the above equation is the desirable output signal and the second and the third terms represent error factors. When the repetition frequency $1/T_0$ of the switch is chosen sufficiently higher beyond the frequency ranges of $e_c(t)$ and $e_{in}(t)$, error factors $\Delta_1(t)$, $\Delta_2(t)$ can be calculated as follows;

$$\begin{aligned}\Delta_1(t) &= \int_{-\infty}^{t} e_{in}(t)\sum_{m=1}^{\infty}\frac{1}{m}\left[-\sin\frac{2\pi}{T_0}mt + \sin\frac{2\pi}{T_0}m\{Me_c(t)+t\}\right]dt \\ &\fallingdotseq e_{in}(t)\sum_{m=1}^{\infty}\frac{T_0}{2\pi m^2}\left[\cos\frac{2\pi}{T_0}mt - \cos\frac{2\pi}{T_0}m\{Me_c(t)+t\}\right]\end{aligned} \tag{16}$$

$$\begin{aligned}\Delta_2(t) = \int_{-\infty}^{t}\int_{-\infty}^{t'} &\left(\frac{M}{T_0}e_c(t') + \sum_{m=1}^{\infty}\frac{1}{m}\left[-\sin\frac{2\pi}{T_0}mt' + \sin\frac{2\pi}{T_0}m\{Me_c(t')+t'\}\right] + \frac{R}{R_{in}}\right) \\ \times &\left(\frac{M}{T_0}e_c(t'') + \sum_{m=1}^{\infty}\frac{1}{m}\left[-\sin\frac{2\pi}{T_0}mt'' + \sin\frac{2\pi}{T_0}m\{Me_c(t'')+t''\}\right]\right)e_{in}(t'')dt''dt'\end{aligned}$$

$$
\begin{aligned}
&=\int_{-\infty}^{t}\int_{-\infty}^{t'}\left(\frac{M}{T_0}\right)^2 e_c(t')e_c(t'')e_{in}(t'')dt''dt' \\
&+\left\{\frac{M}{T_0}e_c(t)+\frac{R}{R_{in}}\right\}\sum_{m=1}^{\infty}\frac{T_0^2}{4\pi^2m^3}\left[-\sin\frac{2\pi}{T_0}mt+\sin\frac{2\pi}{T_0}m\{Me_c(t)+t\}\right] \\
&+\int_{-\infty}^{t}\frac{M}{T_0}e_c(t)e_{in}(t)dt\sum_{m=1}^{\infty}\frac{T_0}{2\pi m^2}\left[\cos\frac{2\pi}{T_0}mt-\cos\frac{2\pi}{T_0}m\{Me_c(t)+t\}\right] \\
&+\int_{-\infty}^{t}\sum_{l=1}^{\infty}\frac{1}{l}\left[-\sin\frac{2\pi}{T_0}lt+\sin\frac{2\pi}{T_0}l\{Me_c(t)+t\}\right] \\
&\qquad\times\sum_{m=1}^{\infty}\frac{T_0}{2\pi m^2}\left[\cos\frac{2\pi}{T_0}mt-\cos\frac{2\pi}{T_0}m\{Me_c(t)+t\}\right]dt
\end{aligned}
\tag{17}
$$

where it is assumed that the initial values of integrations are zero.

$$
\Delta(t)=-\frac{1}{CR}\Delta_1(t)+\frac{1}{(CR)^2A}\Delta_2(t) \tag{18}
$$

$\Delta(t)$ of the above equation (18) represents the total error, displacement from ideal output signal, in the time-amplitude plane. The maximum value of $\Delta(t)$ can be calculated as follows;

$$
|\Delta(t)|\leqq\frac{1}{CR}|\Delta_1(t)|+\frac{1}{(CR)^2A}|\Delta_2(t)| \tag{19}
$$

Using Riemann's ζ function, next inequations are derived,

$$
\begin{aligned}
|\Delta_1(t)|&\leqq|e_{in}(t)|\sum_{m=1}^{\infty}\frac{T_0}{\pi m^2} \\
&\leqq\frac{T_0}{\pi}|e_{in}(t)|\zeta(2)
\end{aligned}
\tag{20}
$$

and

$$
\begin{aligned}
|\Delta_2(t)|&\leqq\left|\int_{-\infty}^{t}\int_{-\infty}^{t'}\left(\frac{M}{T_0}\right)^2 e_c(t')e_c(t'')e_{in}(t'')dt''dt'\right| \\
&+\left|\frac{M}{T_0}e_c(t)+\frac{R}{R_{in}}\right|\sum_{m=1}^{\infty}\frac{T_0^2}{2\pi^2m^3}+\left|\int_{-\infty}^{t}\frac{M}{T_0}e_c(t)e_{in}(t)dt\right|\sum_{m=1}^{\infty}\frac{T_0}{\pi m^2} \\
&+\left|\int_{-\infty}^{t}\frac{T_0}{2\pi m^2}\left[\cos\frac{2\pi}{T_0}mt-\cos\frac{2\pi}{T_0}m\{Me_c(t)+t\}\right]dt\right| \\
&\leqq\left|\int_{-\infty}^{t}\int_{-\infty}^{t'}\left(\frac{M}{T_0}\right)^2 e_c(t')e_c(t'')e_{in}(t'')dt''dt'\right| \\
&+\left|\frac{M}{T_0}e_c(t)+\frac{R}{R_{in}}+1\right|\frac{T_0^2}{2\pi^2}\zeta(3)+\left|\int_{-\infty}^{t}\frac{M}{T_0}e_c(t)e_{in}(t)dt\right|\frac{T_0}{\pi}\zeta(2)
\end{aligned}
\tag{21}
$$

The terms of errors in Eq. (20), the second and the third term in Eq. (21) are caused by the switching operation, and these errors can be eliminated by means of choosing the repetition frequency $1/T_0$ of switch sufficiently higher beyond the frequency ranges of $e_{in}(t)$ and $e_c(t)$. The error of the first term in Eq. (21) cannot be elminated by making T_0 small, but it is able to neglect from Eq. (18) by making the voltage gain A of the operational amplifier sufficiently large.

As the result, the output voltage $e_{out}(t)$ can be expressed in next Eq. (22).

$$e_{out}(t) = -\frac{1}{CR}\frac{M}{T_0}\int_{-\infty}^{t} e_c(t)e_{in}(t)dt \tag{22}$$

From Eq. (22), it is shown the circuit in Fig. 1 has the function of the multiplying integrator.

When the frequency range of external control signal voltage $e_c(t)$ is limited lower enough than that of input signal voltage $e_{in}(t)$, Eq. (22) is reformed as follows;

$$e_{out}(t) = -\frac{1}{CR}\frac{M}{T_0}e_c(t)\int_{-\infty}^{t} e_{in}(t)dt \tag{23}$$

It can be seen from Eq. (23) the circuit in Fig. 1 operates as the controllable coefficient integrator.

The frequency response of the controllable coefficient integrator is shown in Fig. 2. In Fig. 2, $5\,V_{rms}$ sinusoidal voltage and DC parameter voltage are used as the input signal voltage $e_{in}(t)$ and the external control voltage $e_c(t)$ respectively. The solid line shows the theoretical value and the symbol ∘ the measured value. In Fig. 3, the output voltage waveform and the external control voltage waveform are shown. The rectangular wave and the triangular wave are used for the input voltage $e_{in}(t)$ and the external control voltage $e_c(t)$ respectively. The rectangular input voltage $e_{in}(t)$ is integrated to be the triangular wave and its amplitude is controlled by the external control voltage $e_c(t)$ of triangular wave. As the results, the output voltage $e_{out}(t)$ appears as the amplitude modulated triangular wave by the external control voltage $e_c(t)$ of the triangular wave. In this controllable coefficient integrator, the repetition frequency of the switch is chosen at 10 kHz and it operates for about 1 kHz input signal voltage.

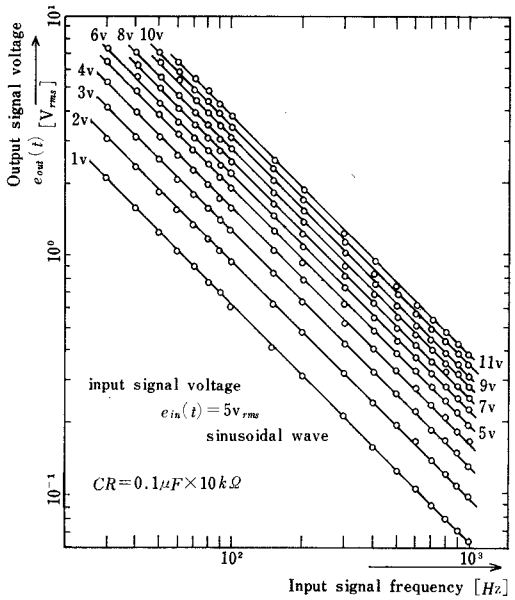

Fig. 2 Frequency response of controllable coefficient integrator

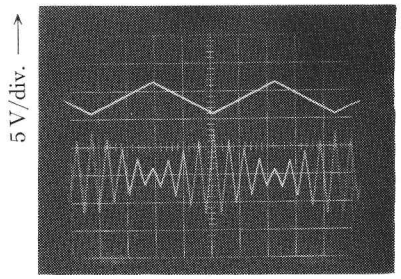

Fig. 3 External control voltage waveform and output voltage waveform of controllable coefficient integrator

3. Application to the controllable parameter filter

When the external control signal voltage $e_c(t)$ varies very slowly compared with the input signal voltage $e_{in}(t)$, the controllable coefficient integrator may be considered to be a circuit having the variable transfer function.[3)]

Fourier transform of the both side of Eq. (23) can be expressed as follows;

$$E_{out}(j\omega, t) = -\frac{1}{CR}\cdot\frac{M}{T_0}\cdot e_c(t)\cdot\frac{1}{j\omega}E_{in}(j\omega, t) \tag{24}$$

The right hand side of Eq. (24) represents the Fourier transform except the external control signal voltage $e_c(t)$. $E_{in}(j\omega, t)$ is Fourier transform of the input voltage $e_{in}(t)$, when $e_{in}(t)$ does not contain $e_c(t)$, it may be expressed $E_{in}(j\omega)$. The variable transfer function $S_0(j\omega, t)$ is defined as follows;

$$S_0(j\omega, t) = E_{out}(j\omega, t)/E_{in}(j\omega,t) = -\frac{1}{CR}\cdot\frac{M}{T_0}\cdot\frac{e_c(t)}{j\omega} \tag{25}$$

Evidently,

$$E_{out}(j\omega, t) = S_0(j\omega, t)E_{in}(j\omega, t) \tag{26}$$

$$e_{out}(t) = \frac{1}{2\pi}\int_{-\infty}^{\infty} S_0(j\omega, t)\cdot E_{in}(j\omega, t)e^{j\omega t}d\omega \tag{27}$$

As the pulse width modulated wave $\kappa_s(t)$ which controls on-off of the switch is modulated linearly by the external control signal $e_c(t)$, the variable transfer function $S_0(j\omega, t)$ contains $e_c(t)$ and varies linearly according to the external control signal voltage $e_c(t)$.

Using the variable transfer function $S_0(j\omega, t)$, the controllable parameter filter is discussed as an application of the controllable coefficient integrator.

3.1 Low pass filter with controllable cut-off frequency

As the representation of the low pass filter, the 2nd order Butterworth filter is discussed. It is constructed as shown in Fig. 4 using the controllable coefficient integrators. The composite variable transfer function $S_B(j\omega, t)$ of this filter is represented as follows;

$$S_B(j\omega, t) = \frac{1}{1/S_0^2(j\omega, t) - \sqrt{2}/S_0(j\omega, t) + 1} \tag{28}$$

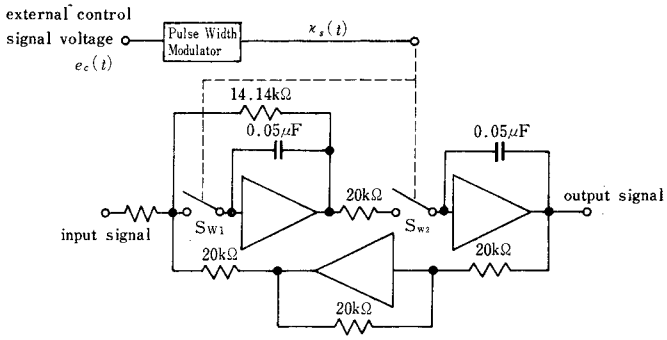

Fig. 4 Low pass filter with controllable cut-off frequency

Substituting Eq. (25) into Eq. (28), it is rewritten as

$$S_B(j\omega, t) = \frac{1}{\left(\frac{CRT_0}{Me_c(t)}\right)^2 (j\omega)^2 + \sqrt{2}\left(\frac{CRT_0}{Me_c(t)}\right) j\omega + 1} \tag{29}$$

and

$$|S_B(j\omega, t)| = \frac{1}{\sqrt{1+\left(\frac{CRT_0}{Me_c(t)}\right)^4 \omega^4}} \tag{30}$$

From Eq. (30), the cut-off angular frequency ω_c of this Butterworth filter is represented by

$$\omega_c = \frac{M}{CRT_0} e_c(t) \tag{31}$$

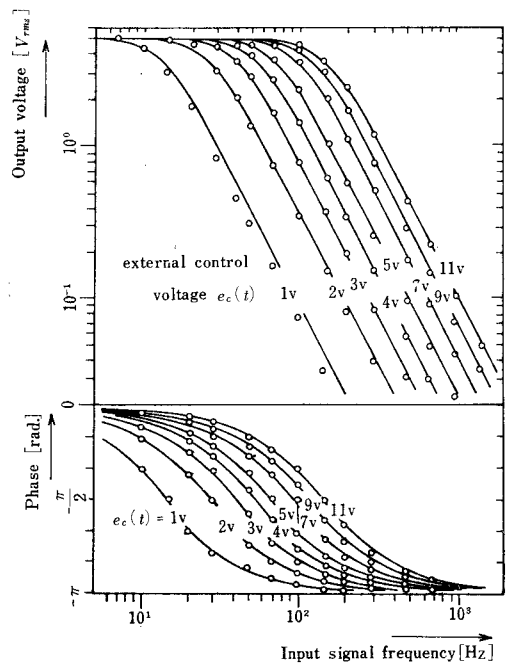

Fig. 5 Frequency response of low pass filter with controllable cut-off frequency

As the results, the cut-off angular frequency ω_c can be controlled linearly by the external control signal voltage $e_c(t)$. The frequency response of this Butterworth low pass filter is shown in Fig. 5 regarding the external control voltage $e_c(t)$ as the parameter. The solid line represents the theoretical value and the symbol ∘ the measured value. The measured value agrees with the theoretical value for practical use.

3.2 Band pass filter with controllable center frequency

As the same manner of Butterworth low pass filter, the band pass filter whose center frequency is controlled by the external control signal voltage $e_c(t)$ can be constructed as in Fig. 6 using controllable coefficient integrators.

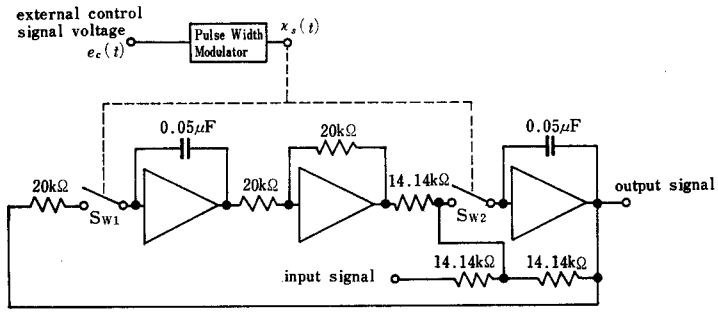

Fig. 6 Band pass filter with controllable center frequency

The composite variable transfer function $S_{bn}(j\omega, t)$ of this band pass filter is expressed as follows;

$$S_{bn}(j\omega, t) = \frac{\sqrt{2}/S_0(j\omega, t)}{1/S_0^2(j\omega, t) - \sqrt{2}\,S_0(j\omega, t) + 1} \tag{32}$$

Substituting Eq. (25) into Eq. (32), it results

$$S_{bn}(j\omega, t) = \frac{-\sqrt{2}\left(\frac{CRT_0}{Me_c(t)}\right)j\omega}{\left(\frac{CRT_0}{Me_c(t)}\right)^2(j\omega)^2 + \sqrt{2}\left(\frac{CRT_0}{Me_c(t)}\right)j\omega + 1} \tag{33}$$

and

$$|S_{bn}(j\omega, t)| = \frac{\sqrt{2}\left(\frac{CRT_0}{Me_c(t)}\right)\omega}{\sqrt{1 + \left(\frac{CRT_0}{Me_c(t)}\right)^4\omega^4}} \tag{34}$$

From Eq. (31), the center angular frequency ω_{cn} of this band pass filter is represented by

$$\omega_{cn} = \frac{M}{CRT_0}e_c(t) \tag{35}$$

As the results, the center angular frequency ω_{cn} of this band pass filter can be controlled linearly by the external control signal voltage $e_c(t)$. The frequency response of this filter is shown in Fig. 7 regarding the external control voltage $e_c(t)$ as the parameter. The solid

line represents the theoretical value and the symbol ∘ the measured value. The measured value agrees with the theoretical value for practical use.

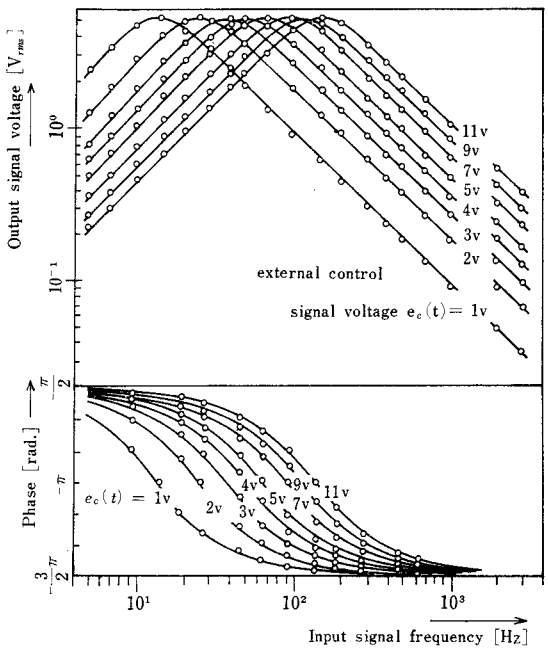

Fig. 7 Frequency response of band pass filter with controllable center frequency

3.3 Auto frequency analyser

When the quality factor Q of the band pass filter shown in Fig. 6 is sufficiently high, sweeping the center frequency of the band pass filter by $e_c(t)$, it may be an auto frequency analyser as the center frequency ω_{cn} can be controlled by the external control signal voltage $e_c(t)$. The block diagram of the auto frequency analyser is shown in Fig. 8. The quality factor Q is improved by making the coefficients of the first order terms of $j\omega$ in Eq. (33) small and by cascading two filters.

The frequency response $S_{at}(j\omega, t)$ of the frequency selective part of this analyser is expressed as follows;

$$S_{at}(j\omega,t)=\left[\frac{0.01\,S_0(j\omega,t)}{1-0.01\,S_0(j\omega,t)+S_0^2(j\omega,t)}\right]^2$$
$$=\left[\frac{0.01\left(\frac{CRT_0}{Me_c(t)}\right)j\omega}{\left(\frac{CRT_0}{Me_c(t)}\right)^2(j\omega)^2+0.01\left(\frac{CRT_0}{Me_c(t)}\right)j\omega+1}\right]^2 \tag{36}$$

and

$$|S_{at}(j\omega,t)|=\frac{0.0001\left(\frac{CRT_0}{Me_c(t)}\right)^2\omega^2}{\left[1-\left(\frac{CRT_0}{Me_c(t)}\right)^2\omega^2\right]^2+0.0001\left(\frac{CRT_0}{Me_c(t)}\right)^2\omega^2} \tag{37}$$

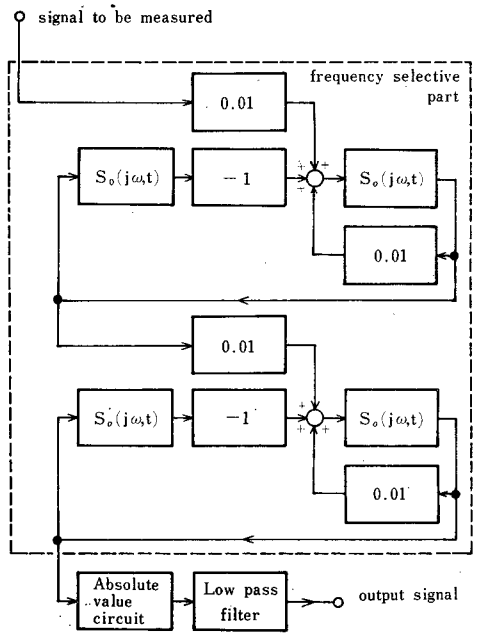

Fig. 8 Block diagram of auto frequency analyser

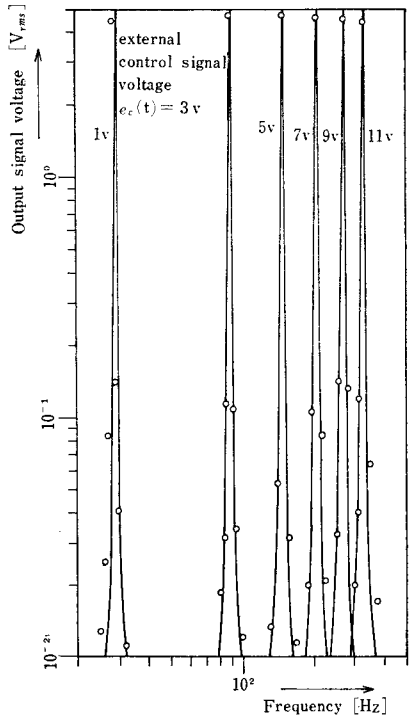

Fig. 9 Frequency response of auto frequency analyser

The center angular frequency ω_{at} of this frequency selective filter is also represented by

$$\omega_{at} = \frac{M}{CRT_0} e_c(t) \tag{38}$$

The output signal voltage of this frequency selective part is detected by absolute value circuit and smoothed by low pass filter, and it becomes the output signal voltage of the analyser. In Fig. 8, the absolute value circuit for detection is constructed with two operational amplifiers and two diodes, and the second order Butterworth filter whose cut-off frequency is 0.5 Hz is used for the smoothing low pass filter.

The frequency response of $S_{at}(j\omega, t)$ is shown in Fig. 9 regarding the external control signal voltage $e_c(t)$ as the parameter. The solid line indicates the theoretical value and the symbol ∘ the measured value.

Experimental results are shown in Fig. 10. The external control signal voltage $e_c(t)$ of 0.001 Hz sinusoidal voltage is employed to sweep the abscissa of the frequency. Fig. 10(a) represents the spectrum of the 35 Hz saw-tooth voltage waveform. The amplitude of the n-th harmonic component reduces to $1/n$ as well-known. Fig. 10(b) represents the spectrum of the amplitude (balanced) modulated waveform whose carrier and modulating signal are 200 Hz sinusoidal voltage and 5 Hz saw-tooth voltage respectively. Experimental results in Fig. 10 indicates this auto frequency analyser is available enough for practical use.

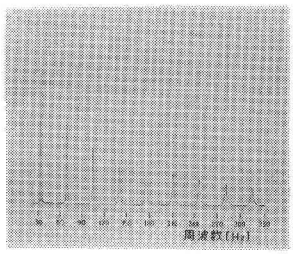

(a)

Spectrum of 35 Hz saw-tooth voltage

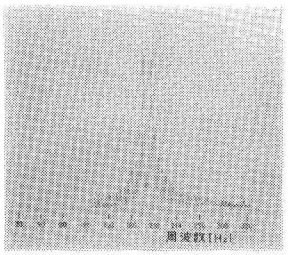

(b)

Spectrum of amplitude modulated signal
carrier signal: 200 Hz sinusoidal voltage
modulating signal: 5Hz saw-tooth voltage

Fig. 10 Analytical results

4. Conclusion

The controllable coefficient integrator using the switching operation is discussed. This circuit may be recognized to be the combination circuit of the integrator and the time-sharing type multiplier. In general, the time-sharing type multiplier requires the smoothing output low pass filter. Combination with the integrator, however, never require it and the controllable coefficient integrator can be realized simply.

The controllable coefficient integrator circuit, which has the series switch in the input terminal, is analysed and the error of the displacement in the time-amplitude plane from the ideal output signal voltage is discussed in detail. The frequency response of this integrator is measured in experiment regarding the external control signal voltage $e_c(t)$ as the parameter, and this circuit may be recognized to be the circuit which realizes the variable transfer function. Using this characteristics, the controllable cut-off frequency low pass filter, the controllable center frequency band pass filter and the auto frequency analyser are constructed. Frequency responses of these circuits are discussed theoretically and experimentally, and the agreement of theoretical and experimental values is examined. Some of periodical voltage waveforms are analysed using the auto frequency analyser and satisfactory results are obtained.

References

1) K. Terasawa, Shizen Kagakusha no tameno Sugaku Gairon, p. 575, Iwanami, (1967).
2) I. Mizoshiri, S. Minamoto and K. Miyakoshi, Trans. IECE, **54-A**, 6 (1971).
3) K. Toda, Kahen Teisu Kairoron, p. 3, Kyoritsu (1960).